iJRASET
International Journal For Research in Applied Science and Engineering Technology

INTERNATIONAL JOURNAL FOR RESEARCH

IN APPLIED SCIENCE & ENGINEERING TECHNOLOGY

Volume: 5 **Issue:** IX **Month of publication:** September 2017

DOI: http://doi.org/10.22214/ijraset.2017.9015

www.ijraset.com

Call: 08813907089 | E-mail ID: ijraset@gmail.com

International Journal for Research in Applied Science & Engineering Technology (IJRASET)
ISSN: 2321-9653; IC Value: 45.98; SJ Impact Factor:6.887
Volume 5 Issue IX, September 2017- Available at www.ijraset.com

Synthesis and Vibrational Spectral Analysis of (E)-N′- (Pyridin-2-Ylmethylene) Isonicotinohydrazide - A Combined Experimental and Theoretical Study

A. Nathiya[1], H. Saleem[2], M. Suresh[3], M. Syed Ali Padusha[4], K. Krishnasamy[5]
[1, 2] *Department of Physics, Annamalai University, Annamalainagar 608 002, Tamil Nadu, India*
[3,4] *PG and Research Dept. of Chemistry, Jamal Mohamed College (Autonomous), Tirchy -620020, Tamil Nadu, India*
[5,] *Department of Chemistry, Annamalai University, Annmalainagar-608 002.*

Abstracts: ***In the present study, a new derivative had been designed by bridge elongation and push–pull strategy from (E)-N'-(Pyridin-2-ylmethylene) isonicotinohydrazide (P2MINH) with the aim to enhance electronic and charge transport properties. The geometrical parameters of the title compound were calculated. The molecular structure, IR and Raman spectra of the isonicotinohydrazide were interpreted by comparing the experimental results with the theoretical B3LYP/6-311++G (d, p) calculations. The data obtained from density functional theory (DFT) computation was used to perform total energy distribution (TED) analysis using scaled quantum mechanics (SQM) method to complement and give insight in the experimental vibrational assignment. The electronic transition was studied using UV-Vis spectrum recorded in the region 200-600nm. The ^{1}H and ^{13}C nuclear magnetic resonance (NMR) chemical shift of the title compound were also calculated. The molecular docking solved the binding mode of 3DL6 complex. This work can serve as a basis for better drug design of highly selective human lanosterol 14-alpha dimethylase in complex with ketoconazole.***

Keywords: FT-IR, FT-Raman, UV, NMR, TED, P2MINH, Docking.

I. INTRODUCTION

Pyridine compounds have been used as non-linear materials and photo chemicals widely used as anti-cancer drugs, anti-fungal reagents, herbicides, plant growth reagents and anti-hypertension, etc [1]. Many substituted pyridines are involved in bioactivities with applications in agricultural products and pharmaceutical drugs [2-4]. The ring nitrogen of most pyridines undergoes reactions such as protonation, acylation and alkylation [3].

It is well known that the hydrazone group exhibits pharmaceutical and anti-microbial activities such as biological actividesl [5], anti-inflammatory [6], anti-convulsant [7], anti-tubercular [8] and anti-leishmanial activities [9]. Hydrozones play an important role in improving the anti-tumor selectivity and toxicity profile of anti-tumor agents by forming drug carrier systems employing suitable carrier proteins [10] as well as used in catalytic processes [11] and waste water treatment [12]. The hydrazones were also shown to be involved in bio-molecular reactions such as cycloadditions and condensations [13, 14]. The benzohydrazide derivatives shows wide spectrum of biological activities such as anti-bacterial [15], anti-fungal [16], anti-tubercular [17] and anti-proliferative [18] activities. The harmonic frequencies of pyridine derivatives were calculated by several authors [19-21].

The vibrational and structural properties of a new pyrazoline derivative viz., 2-(5-(4-Chlorophenyl)-3-(pyridine-2-yl)-4,5-dihydropyrazol-1-yl)benzo[d]thiazole (2CPDBT) had been studied using Gaussian 09 software package. A detailed interpretation of the vibrational spectra of 2CPDBT was reported based on the potential energy distribution. The ^{1}H and ^{13}C NMR chemical shifts of the compound 2CPDBT were calculated using B3LYP/6-311++G(2d,2p) basis set. The theoretical absorption spectrum had been calculated using TD-DFT method and compared with experimental spectrum. The charge delocalization had been analyzed using NBO analysis. The band gap, HOMO & LUMO energies, MEP map and Mulliken atomic charges were also calculated and analyzed [22]. In our previous study, the FT-IR, FT-Raman and UV-Vis spectra of the Schiff base compound (E)-N'-(Pyridin-2-yl) methylene) nicotinohydrazide (P2MNH) had been recorded and analyzed [23]. The optimized molecular structure, vibrational assignments and NMR chemical shift for P2MNH have been investigated using DFT/B3LYP/6-311++G(d,p) level of theory. The NLO, Mulliken atomic charges, HOMO-LUMO energies, MEP surface had been analyzed. Furthermore, we interpreted the

calculated spectra on the basis of TED. To establish information about the interactions between human cytochrome protein and this novel compound, theoretically docking studies were also carried out using Schrödinger software.

Literature survey reveals that neither quantum mechanical calculation nor vibrational analysis for the molecule P2MINH have been made so far. In the present work, our aim is to study the bond parameters, vibrational behavior, NLO activity, electronic transition, NMR chemical shift, atomic charges, MEP map, physio-chemical parameters, thermodynamic parameters and intra-molecular charge transfer (ICT) analysis of P2MINH. Hence we recorded FTIR, FT-Raman, UV-Vis and NMR spectra for P2MINH and also performed the suitable theoretical calculation using B3LYP method with 6-311++G(d, p) basis set. The experimental spectral and DFT results were critically analysed in this paper.

II. FT-IR, FT-RAMAN AND UV-VIS SPECTRA DETAILS

The FT-IR spectrum in the spectral range 400-4000 cm^{-1} was recorded using KBr pellet technique with a FT-IR-Shimadzu spectrometer. The spectrum was recorded at room temperature with a scanning speed of 10 cm^{-1} per minute at the spectral resolution of 2.0 cm^{-1} in the Instrumentation laboratory, Jamal Mohamed College, Tiruchirappalli, Tamilnadu. The FT-Raman spectrum was recorded using the 1064nm line of a Nd: YAG laser as excitation wavelength in the region 50-4000 cm^{-1} on Bruker IFS 66v spectrophotometer equipped with a FRA 106 FT-Raman module accessory and at spectral resolution of 4 cm^{-1}. The FT-Raman spectrum was recorded at SAIF Laboratory, IIT Madras. The UV-Vis absorption spectrum of P2MINH was recorded in the range of 200-500 nm using a Shimadzu – 2600 spectrometer in the Department of Chemistry, Jamal Mohamed College, Tiruchirappalli, Tamilnadu. ^{1}H NMR spectrum was recorded on a Bruker 400 MHz spectrometer and ^{13}C NMR spectrum was recorded on a Bruker 100 MHz spectrometer at Annamalai University, Annamalai Nagar, India. Chemical shift values are reported in parts per million (ppm) and tetramethylsilane was used as internal standard.

III. COMPUTATIONAL DETAILS

Theoretical calculations were carried out using Gaussian 03W [24] package of program. Gaussian 03W has already proved to be an important tool predicting molecular structures, spectroscopic properties and molecular origins of NLO properties [25-29]. We have utilized the gradient corrected density functional theory [30] with three parameter hybrid functional (B3) [31] for the exchange part and the Lee-Parr (LYP) correlation function [32]. To find the exact vibrational behaviour of this molecule the TED analysis was performed on the gas phase. The TED analysis was carried out using VEDA 4 program [33]. The TED calculation, which show the relative contributions of the redundant internal coordinates to each normal vibrational mode of the molecule and thus enable us numerically to describe the character of each mode using scaled quantum mechanical (SQM) program.

IV. EXPERIMENTAL DETAILS

A. Synthesis Procedure

10 mL of ethanolic solution of pyridine-2-carboxaldehyde (1 ml, 0.01 mol) were added to 5 mL of aqueous solution of isonicotinic acid hydrazide (1.37 g, 0.01 mol) and stirred for an hour in the presence of hydrochloric acid to form a white precipitate. The precipitate was washed with water and filtered and again washed with petroleum ether (40–60%) and dried over in a vacuum desicator. The compound was recrystallized from ethanol.

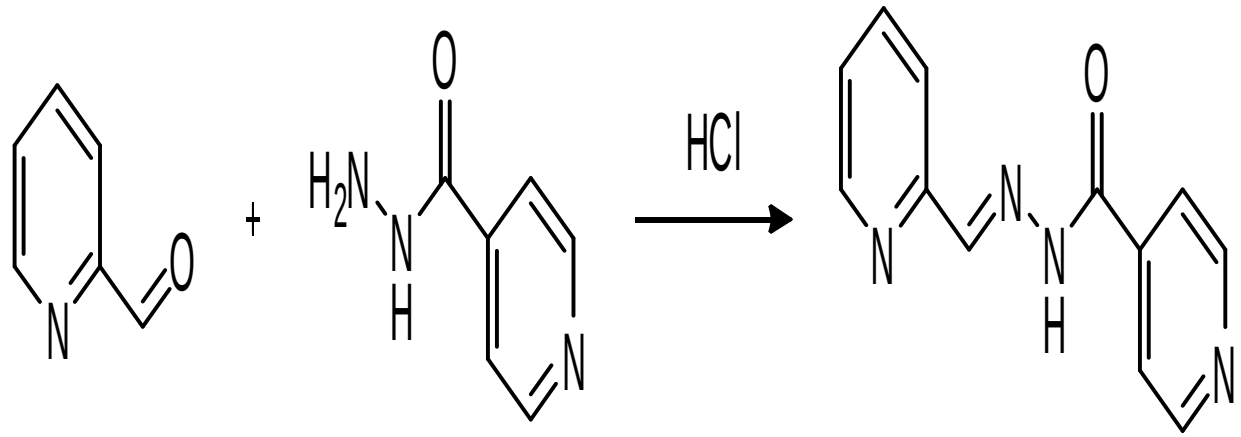

Synthesis of (E)-N′-(Pyridin-2yl-methylene)isonicotinohydrazide

V. RESULTS AND DISCUSSION

A. Molecular Geometry

The optimized structural parameters of P2MINH are calculated using B3LYP/6-311++G(d, p) basis set and are listed in Table 1. The optimized molecular structure as well as atomic numbering is shown in Fig.1. The title molecule has two pyridine rings which are connected by hydrazone linkage. In pyridine ring 1, the bond length of all the C-C bonds is found to be approximately: 1.390Å except the C_4-C_5 bond (1.402Å), which is due to the attachment of hydrogen moiety at C_5 atom. The bond length of C_{16}-C_{21} is positively (0.039Å) deviated from the bond length of C_5-C_{11} (1.468Å), which is due to the carbon atom (C_{16}) of carbonyl group positioned in between nitrogen (N_{14}) and C_{18} on pyridine ring 2. In hydrozone moiety, the nitrogen atom (N_{14}) belongs to N-H group exert a large attraction of the valence electron cloud of the H_{15} atom resulting an increase in the N-H force constant and hence the corresponding (N-H) bond length is decreased (1.016Å) [23] our previous study P2MNH. The calculated bond lengths:C_{16}-N_{14}, C_{11}=N_{13}, N_{13}-N_{14} & C_{16}=O_{17} of hydrozone moiety are 1.386, 1.279, 1.355 & 1.211Å, respectively, which are in line with 1.354, 1.266, 1.375 and 1.224 Å.

In the pyridine ring II, the atoms present in the higher/ lower half regions (C_{20}, N_{22} and C_{25})/ (C_{19}, C_{21} and C_{24}) are accumulated with higher/lower magnitude of electron densities and they exhibit as electron rich/ deficient centres, respectively. On the other hand the alternate fashion of electron rich and electron deficient centres are attributed in the pyridine ring 1. The bond angles C_{21}-C_{24}-H_{26} (119.86˚) and C_{21}-C_{16}-O_{17} (122.24˚) are negatively (~2.47˚ & 1.52˚) deviated from C_{25}-C_{24}-H_{26} and $N_{14}C_{16}O_{17}$, respectively. This represents that the H_{26} atom tilted towards to the atom O_{17} having higher electronegativity. It should be mentioned here that the bond angles are appreciably varied due to the presence of polar carbonyl (C_{16}=O_{17}) group. The calculated bond angle values for C_{11}-C_5-C_4 and C_{11}-C_5-N_6 are 122.25˚ and 114.84˚, respectively, whereas the expected bond angle value would be 120˚. The positive (~2˚) deviation in bond angle (C_{11}-C_5-O_4) is due to the repulsion between C_{11} and C_5 atoms are having negatively charged electron densities. Similarly the negative (~6˚) deviation in bond angle C_{11}-C_5-N_6 is probably due to the attraction between electron rich carbon (C_{11}) and the electron deficient nitrogen (N_6) centres [23]. In pyridine ring 2, the calculated bond angles of C_{16}-C_{21}-C_{19} and C_{16}-C_{21}-C_{24} are 124.14˚ and 117. 95˚, respectively. The expected bond angle value is 120˚ for the same. The positive (~4˚)/ negative (~2˚) bond angle deviations are observed for C_{16}-C_{21}-C_{19}/C_{16}-C_{21}-C_{24}, respectively, which are due to the existence of electron deficient H_{15} and H_{18} atoms/ possible interaction between O_{17} and H_{26} atoms.

In P2MINH, the two pyridine rings are fused by hydrazone linkage. The calculated dihedral angle C_5-C_{11}-N_{13}-N_{14}(-179.43˚), C_{11}-N_{13}-N_{14}-C_{16}(-175.59˚), N_{13}-N_{14}-C_{16}-C_{21}(-178.30˚) are in agreement with the literature values 178.34˚, -176.58˚ and 176.05˚[23].

The calculated dihedral angle for C_5-C_{11}-N_{13}-N_{14}(-179.43˚), N_{13}-N_{14}-C_{16}-C_{21}(178.30˚) indicate that both the pyridine rings are located perpendicular to each other.

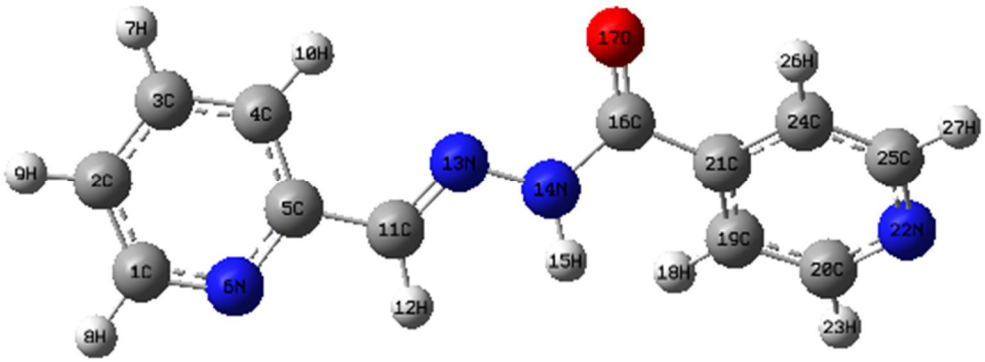

Fig. 1. The Optimized molecular structure of P2MINH

Table. 1. The optimized bond parameters of P2MINH using B3LYP/6-311++G(d, p) level

Parameters	B3LYP/6-311++G(d, p)	XRD [a]
Bond lengths(Å)		
C1-C2	1.393	1.368
C4-C5	1.402	1.384
C5-C11	1.468	1.462
C11-N13	1.279	1.266
N13-N14	1.355	1.375
N14-C16	1.386	1.354
C16-O17	1.211	1.224
C16-C21	1.507	
C19-C20	1.393	
C19-C21	1.397	
C21-C24	1.396	
C24-C25	1.391	
Bond angles(°)		
C4-C5-C11	122.25	122.49
N6-C5-C11	114.84	114. 95
N14-C16-O17	123.76	122.23
O17-C16-C21	122.24	
C16-C21-C19	124.14	
C16-C21-C24	117.95	
C21-C24-H26	119.86	
C25-C24-H26	121.33	
Dihedral angles(°)		
C5-C11-N13-N14	-179.43	-178.34
N13-N14-C16-C21	178.30	

[41] Ramesh Babu et al., (2014) J. Mole. Stuct. 1072 (2014) 84-93.

B. Vibrational Assignments

The molecule under study possesses C_1 point group symmetry. The title compound P2MINH consists of 27 atoms, which makes 75 normal modes of fundamental vibrations, which span the irreducible representations: 51A′+24A″. All the 75 normal modes are active in both Raman and IR absorption. Because of the anharmonicity of the incomplete treatment of electron correlation and the use of finite one-particle basis set, the calculated harmonic vibrational wavenumber are usually higher than the experimental vibrational wavenumbers [35]. The harmonic frequencies are calculated using B3LYP method with 6-311++G(d, p) as basis set. The vibrational assignments are made on the basis of TED result. Furthermore, the none of the predicted vibrational spectra have any imaginary wavenumber, implying that the optimized geometry is located at the local minima on the potential energy surface. The DFT potentials systematically overestimate the vibrational wavenumbers. These discrepancies are corrected by computing anharmonic corrections explicitly (or) by introducing a scaled field (or) directly scaling the harmonic frequencies with the proper factor [36]. Based on this procedure, the harmonic wavenumbers are scaled by the factor (0. 9608) [37, 38]. The experimental and calculated vibrational (IR and Raman) wavenumbers and their probable assignments along with percentage of TED are listed in Table 2. The combined experimental and calculated vibrational spectra are also presented in Figs. 2 and 3.

International Journal for Research in Applied Science & Engineering Technology (IJRASET)
ISSN: 2321-9653; IC Value: 45.98; SJ Impact Factor:6.887
Volume 5 Issue IX, September 2017- Available at www.ijraset.com

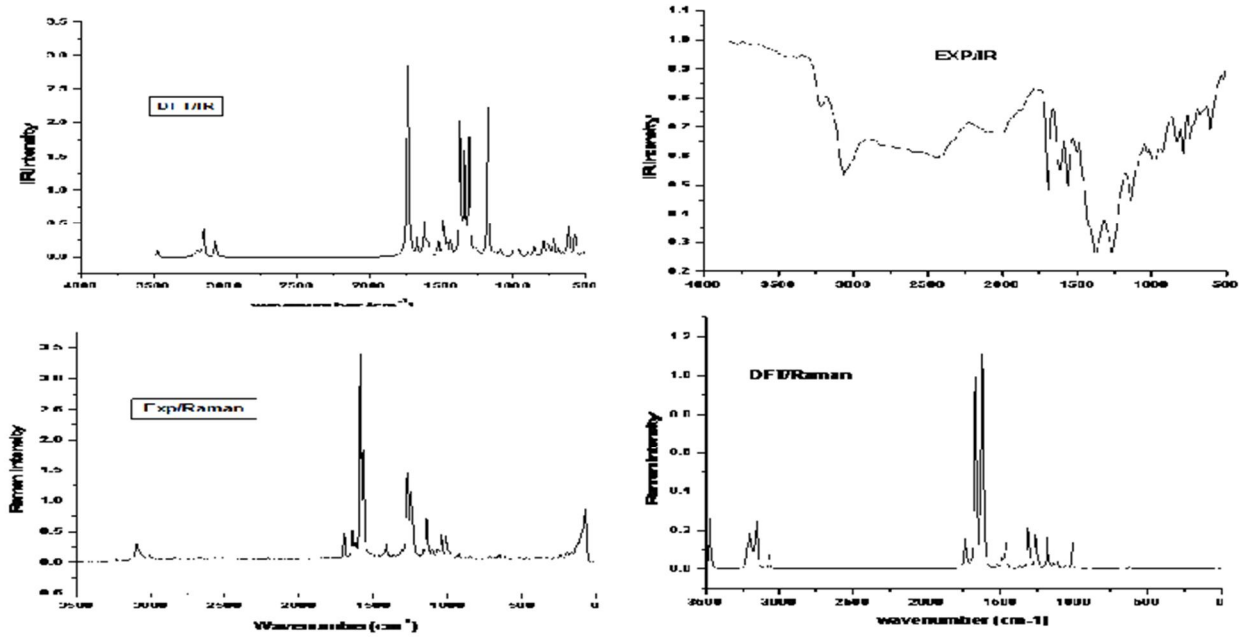

Fig.2.3. The combined Theoretical and Experimental FT-IR, Raman spectra of P2MINH

Table. 2. The experimental and calculated frequencies of P2MINH using B3LYP/6-311++G(d, p) level of basis set [harmonic frequency (cm^{-1}), IR, Raman intensities (Km/mol), reduced masses (amu) and force constants (mdynA°$^{-1}$)]

Mode No	Calculated Frequencies(cm^{-1})		Observed Frequencies(cm^{-1})		IR Intensity		Raman intensity		Reduced Masses	Force Constants	Vibrational Assignments≥10% (TED)[d]
	Un scaled	Scaled[a]	FT-IR	FT-Raman	Abs.	Rel.[b]	Abs.	Rel.[c]			
1	32	31			1.074	0.309	652.282	18.056	4.6697	0.0029	τN$_6$C$_5$C$_{11}$N$_{13}$(21)+ τC$_{24}$C$_{21}$C$_{16}$N$_{14}$(43)+ τC$_{11}$N$_{13}$N$_{14}$C$_{16}$(29)
2	32	31			0.060	0.017	596.168	16.503	5.2203	0.0033	τC$_5$C$_{11}$N$_{13}$N$_{14}$(23)+ τC$_{21}$C$_{16}$N$_{14}$N$_{13}$(55)
3	47	45			1.387	0.399	233.890	6.474	6.1907	0.0081	βC$_5$C$_{11}$N$_{13}$(14)+ βC$_{16}$N$_{14}$N$_{13}$(22)+ βC$_{11}$N$_{13}$N$_{14}$(19)+ βC$_{21}$C$_{16}$N$_{14}$(13)
4	62	60		76w	2.918	0.839	405.523	11.225	5.4109	0.0123	τN$_6$C$_5$C$_{11}$N$_{13}$(23)+ τC$_{24}$C$_{21}$C$_{16}$N$_{14}$(43)
5	118	114			9.647	2.773	68.912	1.908	6.2167	0.0516	βC$_5$C$_{11}$N$_{13}$(18)+ βC$_{11}$C$_5$N$_6$(12)+ βC$_{21}$C$_{16}$N$_{14}$(19)+ ΓC$_{16}$C$_{21}$C$_{24}$C$_{19}$(16)
6	124	120			3.780	1.086	77.842	2.155	6.1758	0.056	τC$_{11}$N$_{13}$N$_{14}$C$_{16}$(29)+ τC$_3$C$_4$C$_5$C$_{11}$(25)
7	177	171			14.281	4.105	65.443	1.812	6.0627	0.1121	τN$_6$C$_5$C$_{11}$N$_{13}$(11)+ τC$_{11}$N$_{13}$N$_{14}$C$_{16}$(14)+ ΓC$_{16}$C$_{21}$C$_{24}$C$_{19}$(35)
8	229	221		196vvw	12.367	3.555	71.970	1.992	3.3687	0.1041	τN$_6$C$_5$C$_{11}$N$_{13}$(16)+ τC$_{21}$C$_{16}$N$_{14}$N$_{13}$(15)+ τC$_3$C$_4$C$_5$C$_{11}$(21)
9	242	235		238vvw	2.494	0.717	60.938	1.687	6.8073	0.2362	βC$_{16}$N$_{14}$N$_{13}$(15)+ βC$_{11}$C$_5$N$_6$(15)
10	259	251			3.933	1.131	53.028	1.468	5.0595	0.2012	βC$_{16}$C$_{21}$C$_{24}$(26)+ βC$_{16}$N$_{14}$N$_{13}$(13)+ βC$_{11}$C$_5$N$_6$(12)
11	321	311			1.491	0.429	20.995	0.581	5.703	0.3468	τC$_1$N$_6$C$_2$C$_3$(13)+ τC$_1$N$_6$C$_4$C$_5$(11)+ τC$_5$C$_{11}$N$_{13}$N$_{14}$(36)+ τC$_{21}$C$_{16}$N$_{14}$N$_{13}$(17)
12	374	362			0.477	0.137	9.822	0.272	8.1395	0.6738	βC$_{19}$C$_{21}$C$_{24}$(21)+ νC$_{16}$C$_{21}$(17)+ βN$_{14}$C$_{16}$O$_{17}$(19)
13	385	373			0.261	0.075	11.328	0.314	2.635	0.231	τC$_{20}$C$_{19}$N$_{22}$C$_{25}$(38)+ τC$_{24}$C$_{20}$C$_{25}$N$_{22}$(27)
14	417	404			6.112	1.757	6.279	0.174	3.6932	0.3795	τC$_3$C$_2$C$_4$C$_5$(62)+ τC$_1$N$_6$C$_4$C$_5$(19)
15	423	410			8.345	2.399	18.911	0.523	5.7822	0.6115	βC$_{21}$C$_{16}$N$_{14}$(16)+ τC$_{24}$C$_{20}$C$_{25}$N$_{21}$(18)

16	490	475	468vw		2.687	0.772	23.106	0.640	6.4552	0.9164	$\beta C_5C_{11}N_{13}(12)+ \beta C_{11}C_5N_6(23)$
17	525	507			1.433	0.412	27.601	0.764	2.2234	0.3613	$\tau H_{15}N_{14}C_{16}C_{21}(22)+ \tau C_1N_6C_2C_3(30)+ \tau C_3C_4C_5C_{11}(12)$
18	536	519	519vw		17.544	5.043	12.536	0.347	2.8783	0.488	$\tau H_{15}N_{14}C_{16}C_{21}(18)+ \tau C_1N_6C_2C_3(22)$
19	547	529			55.732	16.019	147.123	4.073	1.7629	0.3111	$\tau H_{15}N_{14}C_{16}C_{21}(50)$
20	632	612	609w		6.737	1.937	55.038	1.524	7.2786	1.7163	$\beta C_2C_3C_4(57)+ \beta C_2C_1N_6(23)$
21	679	657		648vvw	2.947	0.847	73.385	2.031	5.9078	1.6054	$\beta C_2C_1N_6(21)+ \beta C_4C_5N_6(25)$
22	681	659			1.338	0.385	74.626	2.066	6.791	1.8561	$\beta C_{20}C_{19}C_{21}(25)+ \beta C_{19}C_{20}N_{22}(12)+ \beta C_{24}C_{15}N_{22}(43)$
23	695	673	679vw		54.207	15.581	15.802	0.437	7.3122	2.0853	$\beta N_{14}C_{16}O_{17}(11)+ \beta C_{20}N_{22}C_{25}(36)$
24	719	695			16.336	4.695	14.232	0.394	4.309	1.3134	$\tau C_{20}C_{19}N_{22}C_{25}(16)+ \tau H_{18}C_{19}C_{20}N_{22}(23)+ \Gamma O_{17}C_{21}N_{14}C_{16}(35)$
25	756	732			14.526	4.175	0.520	0.014	2.072	0.6989	$\tau H_9C_2C_1N_6(28)+ \tau H_{10}C_4C_3C_2(29)+ \tau C_1N_6C_4C_5(24)$
26	767	742	744vw		12.691	3.648	37.193	1.030	2.6198	0.9091	$\tau H_{18}C_{19}C_{20}N_{22}(16)+ \tau C_{20}C_{19}N_{22}C_{25}(10)+ \tau C_{24}C_{20}C_{25}N_{22}(10)+ \tau C_{21}C_{24}N_{22}C_{25}(37)+ \Gamma O_{17}C_{21}N_{14}C_{16}(18)$
27	794	768			31.691	9.109	4.577	0.127	1.8368	0.6824	$\tau H_9C_2C_1N_6(21)+ \tau C_3C_2C_4C_5(18)+ \tau C_1N_6C_2C_3(12)+ \tau C_1N_6C_4C_5(24)$
28	849	822	788w		15.394	4.425	7.393	0.205	2.0629	0.878	$\tau H_{18}C_{19}C_{20}N_{22}(36)+ \Gamma C_{24}C_{21}C_{25}H_{26}(10)+ \Gamma O_{17}C_{21}N_{14}C_{16}(14)$
29	860	831	834w	847vvw	4.787	1.376	95.984	2.657	3.8456	1.6758	$\nu C_4C_5(17)+ \nu C_5C_{11}(11)$
30	892	863			2.745	0.789	31.013	0.858	1.2674	0.5946	$\tau H_{18}C_{19}C_{20}N_{22}(24)+ \Gamma C_{24}C_{21}C_{25}H_{26}(59)$
31	917	887			0.070	0.020	2.037	0.056	1.3062	0.6474	$\Gamma C_1C_2C_6H_8(16)+ \tau H_{12}C_{11}N_{13}N_{14}(19)+ \tau H_{10}C_4C_3C_2(51)$
32	942	911			17.602	5.059	87.759	2.429	5.0523	2.6452	$\beta N_{14}C_{16}O_{17}(22)+ \beta C_{16}N_{14}N_{13}(11)$
33	963	932	925vw	924vvw	13.892	3.993	43.605	1.207	1.5215	0.8328	$\tau H_{12}C_{11}N_{13}N_{14}(83)$
34	982	950			0.306	0.088	1.139	0.032	1.351	0.768	$\tau H_{18}C_{19}C_{20}H_{23}(69)+ \tau H_{26}C_{24}C_{25}H_{27}(15)$
35	986	953			3.333	0.958	0.668	0.018	1.4396	0.8251	$\Gamma C_1C_2N_6H_8(66)+ \tau H_9C_2C_1N_6(14)$
36	1007	974			1.428	0.410	2.892	0.080	1.4788	0.8838	$\Gamma C24C21C25H26(11)+ \tau H_{18}C_{19}C_{20}H_{23}(15)+ \tau H_{26}C_{24}C_{25}H_{27}(63)$
37	1009	976			7.365	2.117	813.040	22.506	7.2336	4.343	$\nu N_6C_1(10)+ \nu N_6C_5(11)+ \beta C_2C_3C_4(22)+ \beta C_2C_1N_6(18)+ \beta C_4C_5N_6(14)$
38	1010	977			1.576	0.453	211.333	5.850	6.5657	3.9521	$\nu N_{22}C_{25}(21)+ \nu N_{22}C_{20}(16)+ \beta C_{20}C_{19}C_{21}(17)$
39	1017	984	982w	1009vw	0.222	0.064	3.018	0.084	1.3175	0.8039	$\tau H_9C_2C_1N_6(12)+ \tau H_7C_3C_4H_{10}(75)$
40	1064	1029			4.444	1.277	128.549	3.558	2.2029	1.4695	$\nu C_1C_2(25)+ \nu C_2C_3(34)$
41	1078	1042	1032w	1039vw	5.765	1.657	105.867	2.931	4.5973	3.1502	$\nu N_{14}C_{16}(25)+ \nu N_{13}N_{14}(19)$
42	1092	1056			11.576	3.327	28.745	0.796	1.8913	1.3307	$\beta H_{18}C_{19}C_{21}(15)+ \beta H_{26}C_{24}C_{21}(21)+ \beta C_{19}C_{20}N_{22}(13)+ \beta C_{24}C_{25}N_{22}(11)$
43	1110	1074		1067vw	8.603	2.473	143.492	3.972	1.5885	1.1543	$\beta H_{18}C_{19}C_{21}(16)+ \beta H_{26}C_{24}C_{21}(10)+ \beta C_{19}C_{20}N_{22}(17)$
44	1116	1079			2.200	0.632	28.083	0.777	1.6494	1.2113	$\nu C_3C_4(10)+ \nu C_1C_2(12)+ \beta H_9C_2C_3(20)+ \beta H_{10}C_4C_3(13)$
45	1170	1132		1104vw	245.563	70.581	1492.179	41.306	3.762	3.0366	$\nu N_{14}C_{16}(13)+ \nu N_{13}N_{14}(43)$
46	1173	1134	1138s	1140m	19.145	5.503	294.549	8.154	1.149	0.9327	$\beta H_9C_2C_3(24)+ \beta H_7C_3C_4(32)+ \beta H_{10}C_4C_3(18)$
47	1241	1200			59.820	17.194	977.871	27.069	1.4545	1.321	$\nu N_{22}C_{20}(16)+ \nu N_{22}C_{25}(10)+ \beta H_{23}C_{20}N_{22}(14)+ \beta H_{27}C_{25}N_{22}(11)$
48	1252	1211			98.942	28.438	2390.905	66.184	2.2149	2.0464	$\nu C_{24}C_{25}(13)+ \nu C_{16}C_{21}(13)+ \beta H_{12}C_{11}N_{13}(13)$
49	1260	1219			232.693	66.882	56.189	1.555	2.6622	2.4938	$\nu N_6C_5(11)+ \nu C_{16}C_{21}(11)+ \beta H_{12}C_{11}N_{13}(12)$
50	1278	1237		1244w	31.024	8.917	144.169	3.991	9.3259	8.9873	$\nu N_{22}C_{20}(45)+ \nu C_{21}C_{24}(24)$

51	1303	1260	1265s	1268w	0.057	0.016	212.059	5.870	2.7317	2.734	$\nu N_6C_1(45)+ \beta H_8C_1N_6(13)+ \beta H_{10}C_4C_3(10)$
52	1319	1276			3.553	1.021	608.629	16.848	2.136	2.191	$\nu C_4C_5(16)+ \nu C_5C_{11}(11)+ \beta H_8C_1N_6(15)$
53	1351	1307			0.686	0.197	11.862	0.328	1.3924	1.4989	$\beta H_{18}C_{19}C_{21}(27)+ \beta H_{26}C_{24}C_{21}(25)+ \beta H_{23}C_{20}N_{22}(13)+ \beta H_{27}C_{25}N_{22}(16)$
54	1366	1322			21.487	6.176	59.033	1.634	1.5828	1.7424	$\beta H_8C_1N_6(11)+ \beta H_{12}C_{11}N_{13}(47)$
55	1438	1390	1380s		15.457	4.443	6.739	0.187	1.903	2.3186	$\beta H_{23}C_{20}N_{22}(34)+ \beta H_{27}C_{25}N_{22}(28)$
56	1463	1415		1413vw	35.870	10.310	852.779	23.606	2.1804	2.7519	$\nu N_6C_1(11)+ \nu C_4C_5(10)+ \beta H_9C_2C_3(31)+ \beta H_7C_3C_4(20)$
57	1496	1447			110.461	31.749	304.656	8.433	2.1495	2.8366	$\nu N_6C_5(17)+ \beta H_8C_1N_6(31)+ \beta H_{10}C_4C_3(15)$
58	1519	1469			1.103	0.317	47.539	1.316	2.1142	2.8763	$\beta H_{18}C_{19}C_{21}(13)+ \beta H_{26}C_{24}C_{21}(11)+ \beta H_{23}C_{20}N_{22}(21)+ \beta H_{27}C_{25}N_{22}(23)$
59	1555	1504	1506w		347.916	100.000	716.613	19.837	1.8581	2.6485	$\nu N_{14}C_{16}(12)+ \beta H_{15}N_{14}N_{13}(10)$
60	1596	1543			25.759	7.404	35.944	0.995	7.313	10.9773	$\nu N_{22}C_{25}(32)+ \nu C_{21}C_{24}(32)+ \beta C_{19}C_{20}N_{22}(10)$
61	1606	1553			13.697	3.937	9.238	0.256	5.7128	8.6844	$\nu C_2C_3(33)+ \nu N_6C_5(14)+ \nu C_4C_5(11)$
62	1622	1569	1563s	1567m	16.213	4.660	3612.526	100.000	5.2804	8.1933	$\nu C_3C_4(26)+ \nu C_1C_2(14)$
63	1630	1577		1589s	19.020	5.467	348.790	9.655	5.3392	8.3658	$\nu N_{22}C_{20}(12)+ \nu N_{13}C_{11}(26)+\beta C_{20}N_{22}C_{25}(13)$
64	1674	1619	1613w	1623vvw	2.538	0.730	4370.522	120.982	8.3434	13.7792	$\nu N_{13}C_{11}(75)$
65	1764	1706	1696s	1696w	309.715	89.020	362.475	10.034	11.3643	20.8573	$\nu O_{16}C_{17}(85)$
66	3050	2949			36.114	10.380	32.795	0.908	1.0881	5.9642	$\nu C_{11}H_{12}(100)$
67	3152	3048			15.154	4.356	67.938	1.881	1.0887	6.3747	$\nu C_1H_8(39)+ \nu C_{20}H_{23}(50)$
68	3152	3048			24.857	7.145	58.049	1.607	1.0888	6.3757	$\nu C_1H_8(54)+ \nu C_{20}H_{23}(36)$
69	3158	3054			18.105	5.204	75.347	2.086	1.0907	6.4129	$\nu C_{25}H_{27}(93)$
70	3175	3070	3063s		6.800	1.955	47.005	1.301	1.089	6.4691	$\nu C_2H_9(16)+ \nu C_3H_7(76)$
71	3179	3074			9.719	2.793	55.810	1.545	1.0938	6.5141	$\nu C_{19}H_{18}(88)+ \nu C_{20}H_{23}(11)$
72	3193	3088			14.531	4.177	115.301	3.192	1.0953	6.5823	$\nu C_2H_9(76)+ \nu C_3H_7(14)$
73	3205	3100		3094vw	3.042	0.874	44.013	1.218	1.0935	6.619	$\nu C_{24}H_{26}(97)$
74	3206	3099			2.290	0.658	40.030	1.108	1.0951	6.6322	$\nu C_4H_{10}(89)$
75	3503	3387	3377vw		6.881	1.978	126.946	3.514	1.0763	7.7846	$\nu N_{14}H_{15}(100)$

ν: Stretching, β: in-plane-bending, Γ: out-of-plane bending, τ: Torsion, vw: very week, w: week, m: medium, s: strong, vs: very strong,

a Scaling factor: 0.9608 (Radom et al., 1970 and Pople et al., 1993),

b Relative IR absorption intensities normalized with highest peak absorption equal to 100,

c Relative Raman intensities calculated by Equation (1) and normalized to 100, $Ii = 10\text{-}12 \times (\nu 0\text{-}\nu i)4 \times \frac{1}{\nu i} \times RAi$

d Total energy distribution calculated at B3LYP/6-311++G(d,p) level.

1) *N-H vibrations:* In general, the N-H stretching vibration occurs in the region of 3300-3500cm-1 [39]. The very weak band observed at 3377cm-1 in FTIR spectrum and its corresponding harmonic value 3387cm-1 (mode no:75) is assigned to νN-H vibration. The assignment of the N-H stretching mode is straight forward on the basis of their calculated TED value (100%). The βN-H vibration is assigned to mode no:59 (1504cm-1). This assignment find support from the observed FTIR band 1506cm-1. It should be mentioned here, that this mode is contaminated by νC-N mode and also having considerable TED value (10%). These results are found to be in the same range as in the above literature. On comparing with the literature value, the

down shift of N-H stretching frequency can be attributed to the intermolecular N-H..O interaction. As per the TED result (50%) the computed vibrational wavenunber 529cm-1 (mode no:19) is assigned to τN-H mode and also confirmed by visualizing this mode in Gauss view [03] program. This assignment is in agreement with literature [40]. These assignments are positively (~ 4, 30, 10cm-1) deviated from our earlier assignments (P2MNH)[23], which may be due to the positive magnitude (0.11) of N14 atom creates the possibility of transformation of electron density (ED) from H-15 to N-14. This ED distribution make the N-H bond stronger and hence there is positive deviation. Recently, Ramesh Babu et al., (2014) [41] assigned the νN-H, and βN-H modes respectively to the bands observed at 3349 and 1516 in FTIR spectrum. In our previous study, the medium/weak bands observed at 3373/1476cm-1 in FTIR/FT-Raman spectra were assigned to νN-H and βN-H modes, respectively [23].

2) *C=O vibrations:* The carbon-oxygen double bond is formed by pπ-pπ bonding between carbon and oxygen atoms. Due to the different electronegativities of carbon and oxygen atoms, the bonding electrons are not equally distributed between the two atoms. The following two resonance forms contribute to the bonding of the carbonyl group >C=O↔C+O-. The lone pair of electrons on oxygen also determines the nature on oxygen also determines the nature of the carbonyl group [42]. The stretching vibration of carbonyl group (C_{16}=O_{17}) is expected to occur in the region of 1680-1715cm^{-1} [43, 44]. The medium and weak bands in the FTIR/FT-Raman spectra at 1696cm^{-1} is assigned to C=O stretching mode. This mode is in the expected region and find support from the harmonic value 1706cm^{-1}/mode no:65 in addition to TED value (85%). The $\beta_{C=O}$/$\Gamma_{C=O}$ modes are assigned to mode nos: 32 (911cm^{-1}) / 24 (695cm^{-1}) respectively and also having considerable TED values (22/35%). In P2MINH molecule, the $\nu_{C=O}$, $\beta_{C=O}$ and $\Gamma_{C=O}$ were assigned to harmonic wavenumbers: 1661cm^{-1} (FTIR), 910 and 727cm^{-1} respectively. On comparing the present assignments with earlier study (P2MNH), the positive deviations in stretching, bending modes (~35, 1cm^{-1}) and negative deviation in out-of-plane bending mode (~32cm^{-1}) are due to the distribution of ED around C_{16} atom (-1.10) is greater and hence the possibility of transformation of ED from C_{16} to O_{17} is very appreciable. This process make the C=O bond distance shorter and hence we observed the positive deviation.

3) C-H Vibrations: The hetero aromatic organic compounds commonly exhibit multiple bands in the region of 3000-3100cm^{-1} due to CH stretching vibrations [45]. In this region, the bands are not affected appreciably by the nature of the substituent. The title molecule has eight C-H units and hence eight C-H stretching/in-plane/out-of-plane bending vibrations are possible. The harmonic frequencies lie at 3099, 3100, 3088, 3074, 3070, 3054, 3048, 3048 cm^{-1} (mode nos:74-67) are assigned to C-H stretching modes. These modes are pure modes and their TED contribution is >89%. These assignments are within the expected region and also find support from the observed experimental bands: 3094, 3004 (FT-Raman) and 3063cm^{-1} (FTIR). In P2MNH, the νC-H vibrations were observed in the range 3080-3017cm^{-1}. It should be mentioned here, that the νC-H modes belong to P2MINH are positively deviated from earlier study [23]. In aromatic compounds, the presence of C-H in-plane/out-of-plane bending vibrations appear in the regions 1000-1300cm^{-1}/750-1000cm^{-1}, respectively [46, 47]. The bands observed in FTIR/FT-Raman spectra at 1265, 1138/1413, 1268, 1140, 1067 and its corresponding harmonic values in the range 1469-1074cm^{-1} (mode nos: 58-56, 53, 51, 46, 44, 43) are assigned to β_{C-H} modes. Similarly the calculated frequencies in the range 974-822cm^{-1} (mode nos: 36, 35, 31, 30, 28) and the FTIR band at 847cm^{-1} are assigned to ΓC-H modes. These assignments are having considerable TED value (>10%) and also find support from the literature values 925, 784/997, 923[23]. In P2MNH, the βC-H/ΓC-H modes were assigned in the regions 1448-1090/999-727cm^{-1}, respectively [23]. In this study, some of the βCH and ΓCH modes are positively and negatively deviated, respectively from the previous study [23].
According to Bharani et al., (2015) [48] the ν_{C-H}, β_{C-H} and Γ_{C-H} modes were assigned at 2919/1315 and 910cm^{-1}, respectively in the case of (E)-N'-(furan-2-ylmethylene) nicotinohydrazide. In P2MNH, the above modes were assigned at 2931, 1314 and 947cm^{-1} [23]. Based on the above assignments, the calculated frequencies at 2949, 1322 and 932cm^{-1} (mode nos:66, 54 and 33) are found to have TED values 100, 47 and 83%, respectively from C_{11}-H_{12} modes in P2MINH and hence they are undoubtedly assigned to νC-H, βC-H and τC-H modes. On comparing with previous study (P2MNH)[23], the positive (~18, 8cm^{-1}) and negative (~15cm^{-1}) deviations in stretching, in-plane and out-of-plane bending of C_{11}-H_{12} are observed, respectively.

4) *C-C vibrations:* The ring C=C and C-C stretching vibrations known as semicircle stretching usually occurs in the region1400-1625cm^{-1} [49, 50]. According to Lorence et al., (2012) [51] the νC-C vibrations belong to pyridine ring are usually observed in the ranges of 1470-1510, 1560-1580 and 1590-1640cm^{-1}. For some substituted pyridines, Krishnakumar et al., (2006) [52] assigned the C-C stretching absorption in the region 1218-1668cm^{-1}. In the present investigation, the harmonic frequencies 1569, 1553, 1543, 1276, 1237, 1211, 1079 and 1029cm^{-1} (mode nos:62-60, 52, 50, 48, 44 and 40) are ascribed to νC-C

vibrations. The medium to very weak bands observed at 1567/1563 (FTIR), 1244, 1009cm^{-1} in FT-Raman spectra support above assignments. The TED corresponding to these modes are not pure mode (>13%). For the same mode the harmonic frequencies in the range 1564-1022cm^{-1} were assigned to ν(C-C) vibrations of pyridine rings in P2MNH [23]. According to TED results, the harmonic frequencies near 1276, 1219cm^{-1} (mode nos: 52, 49) are designated as νC_5-C_{11}, νC_{16}-C_{21} modes, respectively. These modes are having considerable TED value (>11%) and also find support from previous study (νC_2-C_{11}: 1267; νC_{18}-C_{16}:1217cm^{-1}) [23]. The CCC in-plane and out-of-plane bending modes associated with smaller force constant than the stretching one and hence assigned to lower frequencies. In general, the characteristic CCC in-plane and out-of-plane bending modes are observed in the range of 700-400cm^{-1} [53, 54]. The β_{CCC}/Γ_{CCC} modes of P2MNH were attributed to harmonic bands:1016, 974, 881, 655, 608/763, 401cm^{-1}, respectively [23]. In this work, the bands arising from β_{CCC}/τ_{CCC} modes of P2MIMH are assigned to FTIR bands at 609/788cm^{-1} and their corresponding harmonic frequencies are 977, 976, 659, 612/768, 404 cm^{-1} (mode nos: 38, 37, 22, 20/27,14) respectively. The harmonic wavenumbers 1276, 1219cm^{-1} (mode nos: 52, 49) are attributed to νC_5-C_{11}, νC_{16}-C_{21} modes. In this study, we observed small positive deviations in νC-C, CCC in-plane and out-of-plane bending modes on comparing with previous study [23].

5) *C=N, C-N and N-N vibrations :* In general, the identification of carbon-nitrogen vibrations is a difficult task, since they full in the complicated region of the vibrational spectrum and mixing of several bands are possible in the region [55]. The C=N/C-N stretching modes appear in the range 1670-1600/1382-1266cm^{-1}, respectively [56, 53]. The νC=N/νC-N vibrations belong to P2MNH were attributed to FT-Raman bands at 1606/1476cm^{-1}, respectively [23]. In hydrazone moiety the calculated (1619/1504cm^{-1}) (mode nos: 64/59) as well as observed wavenumbers 1613/1506cm^{-1} (FTIR) for νC_{11}=N_{13}/νC_{16}-N_{14} modes are in moderate agreement with our previous study [P2MNH] [23]. These assignments are further supported by TED results (75, 12%). The mode no: 59 is not a pure mode and mixed with βNNH mode. The title molecule has two pyridine rings and hence four νC-N modes are possible. The νC_5=N_6, νC_1-N_6 and νC_{20}=N_{22}, νC_{25}-N_{22} modes are assigned to harmonic frequencies at 1553, 1260, 1577 and 1200cm^{-1} (mode nos:61, 51, 63 and 47), respectively. These results are supported by the observed FT-Raman bands: 1589 and 1268 cm^{-1}. As it is evident from the Table 2, the TED values confirm that those vibrations are mixed modes of ν_{CC}, β_{CCH} and β_{CNC} vibrations, respectively and their contributions are 14, 45 and 12%. In P2MNH, the νC_2=N_1/νC_6-N_1 and νC_{25}=N_{23}/νC_{20}-N_{23} modes were assigned to harmonic wavenumbers 1543/1252 and 1542/1240cm^{-1}, respectively [23]. These assignments are positively deviated from our earlier assignments [23]. The harmonic/observed bands established at 673/679 (FTIR) and 1074, 976, 659, 657/1067, 648cm^{-1} (FT-Raman) (mode nos:23 and 43, 37, 22, 21) are respectively assigned to β_{CNC} and β_{CCN} modes of pyridine rings. Similarly the calculated frequencies 1469, 1447, 1390, 1307cm^{-1} (mode nos: 58, 57, 55, 53) are attributed to β_{NCH} mode. The calculated TED corresponding to these modes are not pure with >17%. The assignment of wavenumbers calculated at 768, 742, 519, 373 and 410, 404cm^{-1} (mode nos: 27, 26, 18, 13 and 15, 14) are respectively attributed to τ_{CCNC} and τ_{CCCN} modes. The theoretically computed values for τ_{NCCH} and τ_{HCCH} modes for both pyridine moieties come out to be 863, 822, 768, 732 and 984, 974, 950cm^{-1} (mode nos: 30, 28, 27, 25 and 39, 36, 34), respectively. These modes are having considerable TED values (>22, 18, 21, 75%). Literature survey reveals that the νN-N mode was assigned at 1128/1137cm^{-1} in IR/Raman spectra with medium intensity [57]. In P2NMH [23], the same mode was observed as medium/weak intense bands at 1137/1130cm^{-1} in FTIR/FT-Raman spectra, respectively. Based on the above conclusions, the harmonic wavenumber 1132cm^{-1} (mode no:45) and observed very weak band at 1104cm^{-1} in FT-Raman spectrum is undoubtedly assigned to νN_{13}-N_{14} mode. This assignment is supported by TED value (43%). The present assignment is negatively (~ 26cm^{-1}) deviated from the earlier assignment [23]. According to the TED value, the calculated wavenumbers identified at 1322, 475, 410, 235 and 877, 311, 311, 120cm^{-1} (mode nos: 54, 16, 15, 9 and 31, 11, 11, 6) are ascribed to βN_{13}-C_{11}=H_{12}, βC_5-C_{11}-N_{13}, βC_{21}-C_{16}-N_{14}, βC_{16}-N_{14}-N_{13} and $\tau H_{12}C_{11}N_{13}N_{14}$, $\tau C_5C_{11}N_{13}N_{14}$, $\tau C_{21}C_{16}N_{14}N_{13}$, $\tau C_{11}N_{13}N_{14}C_{16}$, respectively. The mode nos:16, 9 are supported by observed FTIR:468/FT-Raman: 238cm^{-1} bands.

C. NMR analysis

NMR spectroscopy is the key to reveal the conformational analysis of organic molecules. The experimental ^{1}H and ^{13}C NMR spectra of P2MINH have been recorded in DMSO-d_6 and shown in Figs. 4 a and b, respectively. The optimized structure of P2MINH was used to calculated the NMR spectra using GIAO method with B3LYP with 6-311++G(d, p) basis set. The chemical shifts same are reported in ppm relative to TMS for ^{1}H and ^{13} C NMR spectra and are listed in Table 3

. Table 3. Experimental and calculated ^{1}H and ^{13}C chemical shift (ppm) values P2MINH

Hydrogens	Theoretical	Experimental	Carbons	Theoretical	Experimental
H12	8.11	7.83	C16	197.97	161.29
H15	7.62	6.81	C11	162.91	159.35
Ar-H	7.60-8.50	6.36-7.54	C5	152.43	158.06
			C25	150.77	151.66
			C20	150.35	148.76
			C1	148.84	143.76
			C3	138.07	140.28
			C21	137.52	140.05
			C2	123.13	135.85
			C24	119.08	114.37
			C19	119.04	114.04
			C4	118.18	113.72

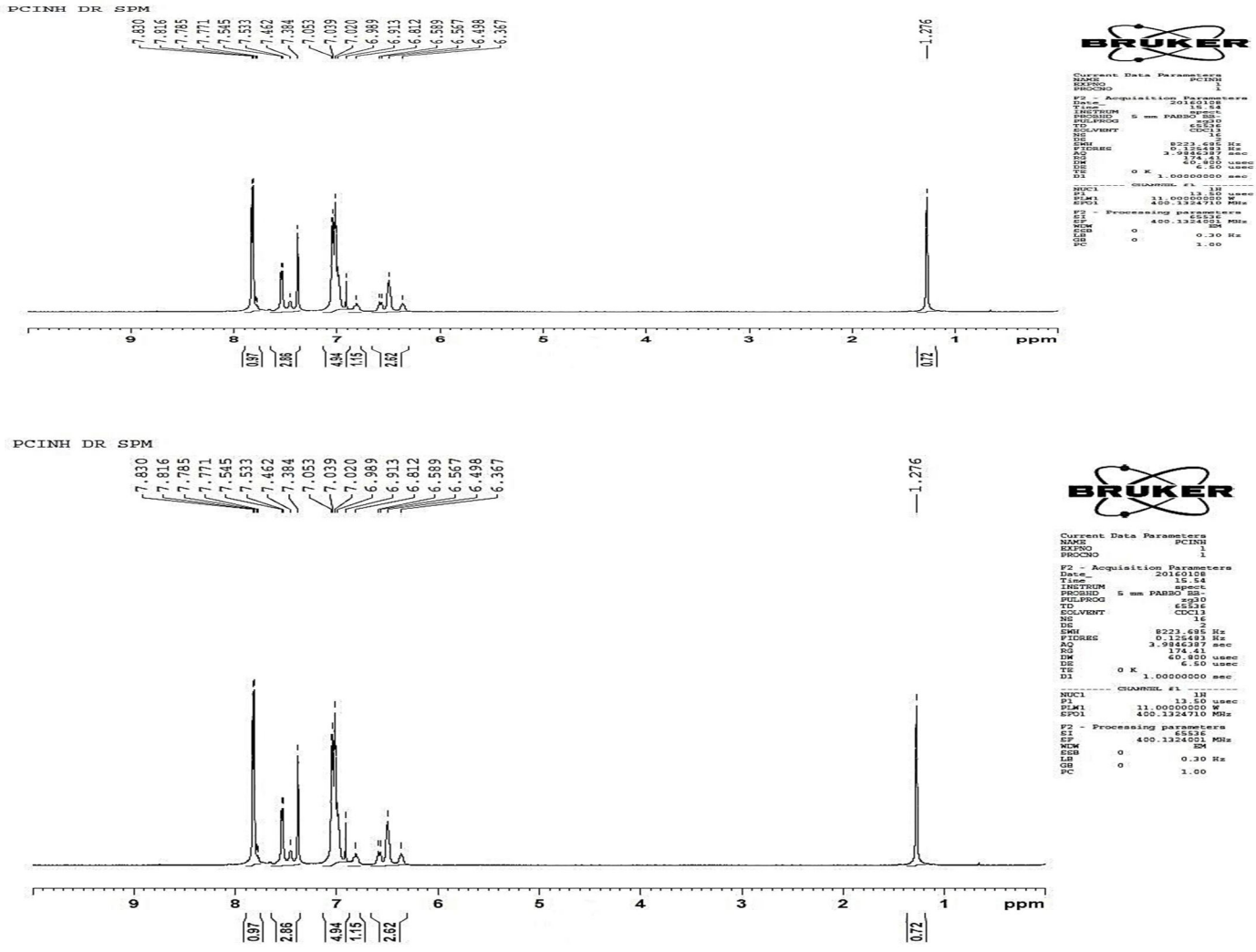

Fig. 4a.b ^{1}H, ^{13}C NMR spectrum of P2MINH

The title molecule has totally twelve carbons; these carbons have shown twelve signals in ^{13}C-NMR spectrum. The signal observed at 161.29 ppm is corresponds to the carbon having strong electronegative atom with it. The carbon bonded with nitrogen atom has shown signal in the deshielded region at 159.35 ppm and its corresponding theoretical signal appeared at 162.91 ppm, respectively. The remaining aromatic carbons in the two pyridine rings are observed in the spectral region of 158.06-113.72 ppm and it's computed chemical shift values are in the spectral range of 152.43-118.18 ppm. From the ^{1}H-NMR spectrum, the protons of the P2MINH has been examined precisely with the help of theoretical chemical shifts. The strong peak observed at δ 7.83 ppm corresponds to the azomethine proton present in the title molecule. It shows good agreement with the chemical shift value computed at δ 8.11 ppm. The N−H proton shows singlet at δ 6.81 ppm in ^{1}H-NMR spectrum and its chemical shift calculated at 7.62 ppm, respectively. The protons present in the two pyridine rings have been observed in the spectral range of 6.36- 7.54 ppm, whereas its corresponding theoretical chemical shifts are in the range 7.60-8.50ppm. The calculated chemical shift values are in agreement with the observed chemical shift values.

D. UV-Vis Spectra

The frontier molecular orbital calculations are carried out using TD-DFT/B3LYP/6-311++G(d, p) method. The calculated results such as the oscillator strength (f), vertical excitation energies, absorption and experimental wavelengths are listed in Table 4. The observed and simulated UV–Vis spectra are shown in Fig 5. Typically, according to the Frank-Condon principle, the maximum absorption peak (λ_{max}) in a UV-Vis spectrum corresponds to vertical excitation. The theoretical calculation predicts one intense electronic transition at 349 nm with an oscillator strength f = 0.0574 is in agreement with the observed experimental data λ_{exp} = 356 nm. This electronic absorption corresponds to the transition from the ground to the first excited state and is mainly described by one electron excitation from the HOMO to the LUMO. Similarly an electronic transition at 317nm with an oscillator strength f=0.0076 is in agreement with observed data (298nm). These two transitions are assigned as π-π*. From the three excitations two have negligible oscillator strengths f < 0.01. The oscillator strength (f) reflects the strength of the particular transition; in other words the light harvesting efficiency. This interesting property is calculated using the expression: light harvesting efficiency =1-10^{-f} and also listed in Table 4.

The light harvesting efficiency of P2MINH is calculated as 0.6701, which represents the capability to capture photons and exhibiting the photon-energy conversion efficiency. Hence this title molecule also have sensitizing application in dye sensitized solar cells. The second absorption maxima observed at 356 nm in chloroform which corresponds to the π-π * transition.

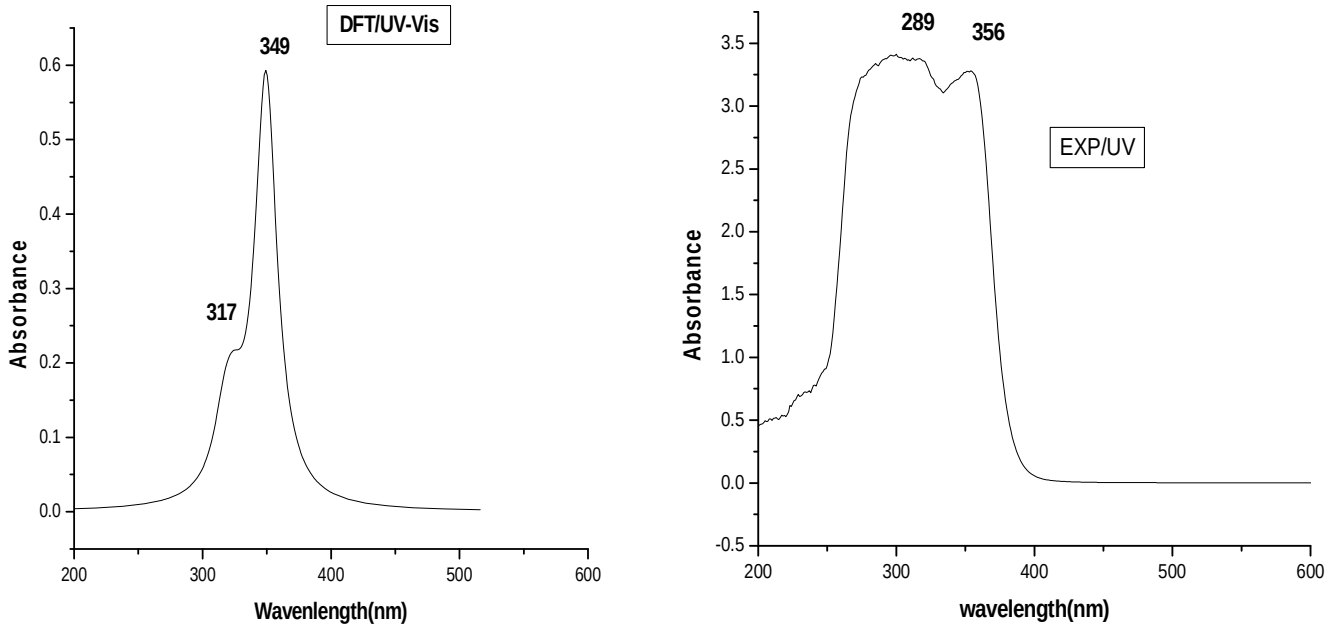

Fig. 5. The combined Theoretical and Experimental UV-Vis spectra of P2MINH

Table 4. The electronic transition of P2MINH

Calculated at B3lyp/6-311++g(d, p)	Oscillator strength	Calculated Band gap(eV/nm)	Experimental Band gap(eV/nm)	
Excited State-1	Singlet-A(f=0.0574)	3.5496eV/349.29nm	356	π-π*
54 -> 60	-0.14888			
56 -> 60	-0.15173			
59 -> 60	0.61914			
59 -> 61	-0.12074			
Excited State-2	Singlet-A(f=0.0080)	3.8266 eV/324.01 nm		
54 -> 60	-0.10838			
56 -> 61	-0.12822			
57 -> 60	-0.43202			
57 -> 61	-0.10158			
58 -> 60	-0.21074			
59 -> 61	0.42885			
Excited State-3	Singlet-A(f=0.0076)	3.9111eV/ 317.00nm	298	π-π*
54 -> 60	-0.19939			
56 -> 61	-0.10777			
57 -> 60	0.43486			
57 -> 61	0.12594			
58 -> 61	0.17777			
59 -> 61	0.38742			

E. Molecular Docking studies

Docking studies are carried out to evaluate the binding affinity and the interactions between the synthesized compound and the human lanosterol 14-alpha dimethylase in complex with ketaconazole (3LD6). The docking score of the different conformer of compound P2MINH ranging from -6.9 to -6.2 kcal/mol in 3LD6 protein. The docking results clearly indicate that the tested compound display one type of interaction. The 2D and 3D view of protein-ligand interactions are shown in Fig 6. The ligand is surrounded by hydrophilic interactions with the amino acids like PHE 234, TYR131, ILE377, ALA311, MET380, LEU308, MET304, LEU159, PHE152, VAL143, PHE139 and ALA144. The TYR145 amino acid interacts with hydrazone moiety via hydrogen bonding interaction with the bond distance 2.14 Å. The protein-ligand interaction value indicates that the synthesized compound P2MINH exhibits better anti-bacterial activity.

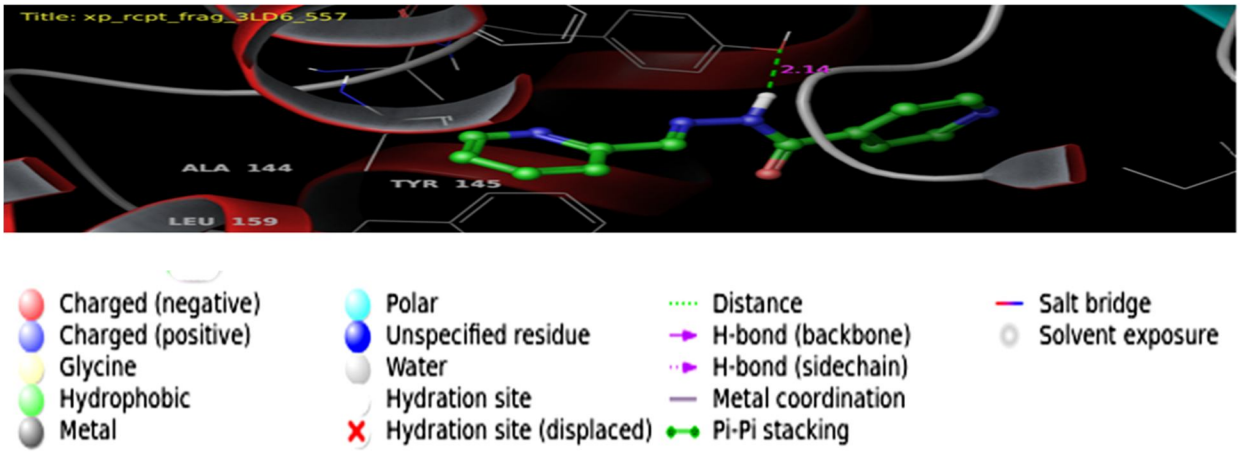

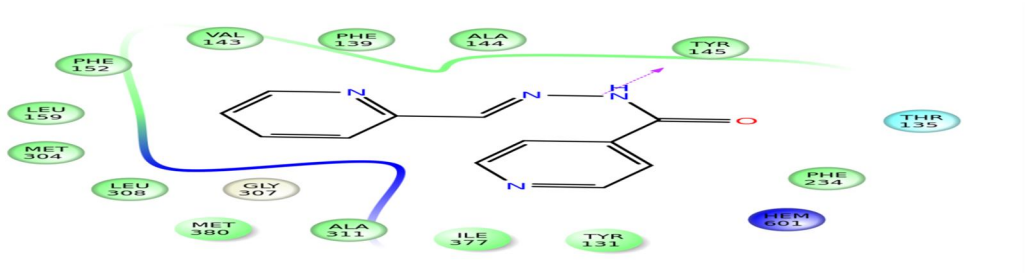

Fig. 6. 2d and 3d interaction of compound P2MINH

VI. CONCLUSIONS

The FT-IR, FT-Raman, NMR and UV-Vis spectra of P2MINH were recorded and analyzed. Most of the recorded vibrational wavenumbers were in agreement with computed wavenumbers. In P2MINH, both the pyridine rings are located perpendicular to each other on comparing the calculated dihedral angle C_5-C_{11}-N_{13}-N_{14}(-179.43˚), N_{13}-N_{14}-C_{16}-C_{21}(-178.30˚). In this study, the positive deviation observed in νC-H, βC-H vibrations and negative deviations observed in ΓC-H and νN-N vibrations, even though both P2MNH and P2MINH are having the same structural arrangements. The positive and negative deviations observed in bond frequency values are due to the different spatial arrangement of the pyridine rings. The molecular docking studies indicate the interaction between the ligand P2MINH with the 3LD6 protein and the Glide score values concluded that the target molecule P2MINH is the better candidate for anti-bacterial activity.

REFERENCES

[1] M.Y. Li, P.Z. Hu, W.R. Zhu, K.X. Xu, Chin. Chem. Lett. 14 (2003) 572–574.
[2] S.P. Jose, S. Mohan, Spectrochim. Acta 64A (2006) 240–245.
[3] K. Othmer, Encyclopedia of Chemical Technology, 4th ed., vol. 20, 1997.
[4] P. Pierrat, P.C. Gros, Y. Fort, J. Comb. Chem. 7 (2005) 879–88
[5] M.T. Cocco, C. Congiv, V. Lilliu, V. Onnis, Bioorg. Med. Chem. 14 (2006) 366–372.
[6] J. Patole, U. Sandbhor, S. Padhe, D.N. Deobagkar, C.E. Anson, A. Powell, Bioorg. Med. Chem. Lett. 13 (2003) 51–55.
[7] P. Vicini, F. Zani, P. Cozzini, I. Doytchinova, Eur. J. Med. Chem. 37 (2002) 553–564.
[8] J. Easmon, G. Pverstinger, G. Heinish, J. Hofmann, Int. J. Cancer 94 (2001) 89–96.
[9] A. Walcourt, M. Loyevsky, D.B. Lovejoy, V.R. Gordeuk, D.R. Richardson, Int. J Biochem. Cell Biol. 36 (2004) 401–407
[10] F. Kratz, V. Beyer, T. Roth, N. Tarasova, P. Collery, F. Lechenault, A. Cazabat, P. Shumacher, C. Unger, U. Falkem, J. Pharm. Sci. 87 (1998) 338–346.
[11] M.S. Niasari, A. Amiri, Appl. Catal. 290 (2005) 46–53
[12] M.G. El-Meligy, S.E. El-Rafie, K.M. Abu-Zied, Desalination 173 (2005) 33–44.
[13] N.P. Belskaya, W. Dehaen, V.A. Bakulev, Arkivoc (i) (2010) 275–332.
[14] S. Dadiboyena, A. Nefzi, Eur. J. Med. Chem. 46 (2011) 5258–5275
[15] R.P. Bhole, K.P. Bhusari, QSAR Comb. Sci. 28 (2009) 1405–1417
[16] C. Loncle, J.M. Brunel, N. Vidal, M. Dherbomez, Y. Letourneux, Eur. J. Med. Chem. 39 (2004) 1067–1071.
[17] K.K. Bedia, O. Elcin, U. Seda, K. Fatma, S. Nathaly, R. Sevim, A. Dimoglo, Eur. J. Med. Chem. 41 (2006) 1253–1261
[18] K.K.V. Raj, B. Narayana, B.V. Ashalatha, N.S. Kumari, B.K. Sarojini, Eur. J. Med. Chem. 42 (2007) 425–42
[19] K.B. Wiberg, V.A. Walters, K.N. Wong, S.D. Colson, J. Phys. Chem. 88 (1984) 6067–6075.
[20] T. Yamamoto, R. Mitsuhashi, M. Akiyama, Y. Kakiuti, J. Mol. Spectrosc. 117 (1986) 30–37.
[21] A. Destexhe, J. Smets, L. Adamowicz, G. Maes, J. Phys. Chem. 98 (1994) 1506– 1514.
[22] Diwaker, Spectrochim. Acta A 128 (2014) 819–829.
[23] A. Nathiya, H. Saleem, S. Bharanidharan, M. Suresh, M. Syed Ali Padusha, Internation. Lett. Chem, Phy. Astro. 61 (2015) 160-175.
[24] M.J. Frisch, Gaussian Inc., Wallingford, CT, 2004.
[25] A. Ben Ahmed, H. Feki, Y. Abid, H. Boughzala, A. Mlayah, J. Mol. Struct. 888 (2008) 180–186.
[26] H. Unver, A. Karakas, A. Elmali, J. Mol. Struct. 702 (2004) 49–54.
[27] Daniel. Glossman-Mitnik, J. Mol. Struct. (THEOCHEM) 808 (2007) 81–84.
[28] P. Srinivasan, T. Kanagasekaran, R. Gopalakrishnan, Spectrochim. Acta 71 (2008) 592–596.
[29] A. Karakas, A. Elmali, Huesyin, Unver, Spectrochim. Acta A 68 (2007) 567–572.
[30] P. Hohenberg, W. Kohn, Phys. Rev. 136 (1964) B864–B871.
[31] A.D. Becker, J. Chem. Phys. 98 (1993) 5648–5652.
[32] C. Lee, W. Yang, R.G. Parr, Phys. Rev. B 37 (1988) 785–789.
[33] M.H. Jamroz, “Vibrational Energy Distribution Analysis”, VEDA 4, Warsaw, 2004.
[34] E.D. Glendering, A.E. Reed, J.E. Carpenter, F. Weinhold, NBO Version 3.1. TCI, University of Wisconcin, Madison, 1998.

[35] M. Szafran, A. Katrusiak, J. Koput, Dega-Szafran, X-ray, MP2 and DFT studies of the structure, vibrational and NMR spectra of homarine , J. mol. struct.846 (2007) 1-12.
[36] M.A. Palafox, Int. J. Quant. Chem. 77 (2000) 661–684.
[37] L. Radom, Scaling Fators for obtaining vibrational Frequencies and zero-point energy from HF/6-31G* and mp2/6-31G*, Harmonic Frequencies", Instrum. J.Chem.33 (1993) 345-350.
[38] J.A. Pople, M. Head-Gordon, K. Raghavachari, J. Chem. Phys. 87 (1987) 5968.
[39] L.J. Bellamy, The infrared spectra of complex molecules, Vol. 2 Chapman and Hall. London (1980).
[40] G. Socrates, Infrared and Raman Characteristic Group Frequencies, third et., Wiley, New York (2001).
[41] N. Ramesh Babu, S. Subashchandrabose, M. Syed Ali Padusha, H. Saleem, V.Manivannan, Y.Erdogdu, J. Mole. Stuct. 1072 (2014) 84-93.
[42] D.N. Sathyanarayanan, Vibrational spectroscopy theory and Applications (2000) 446-447.
[43] N.P.G. Roeges, A Guide to the Complete Interpretation of Infrared Spectra of Organic Structures, Wiley, New York (1994).
[44] M. Barathes, G.D.Nunzio, M. Ribet, Polarrons or Proton transfer in chains of peptide gropus, Synth. Met. 76 (1996) 337-340.
[45] M. Silverstein, C.G. Basseler, C.Morill, spectrometric Identification of Organic compounds, Wiley, New York, 1981.
[46] G. Varsanyi, Assignments of vibrational spectra of 700 Benzene Derivatives, Wiley, New York (1974).
[47] D.N. Sathyanarayanan, Vibrational spectroscopy theory and Applications (2000) 446-447.
[48] S.Bharanidharan, H.Saleem, S.Subashchandrabose, M.Suresh, A.Nathiya, M.Syed Ali Padusha" J. New develop. Chem. 1:2 (2016) 1-25.
[49] V. Krishnakumar, R. John Xavier, Indian J. Pure Appl. Phys., 41 (2003) 95.
[50] K. Furic, V. Mohacek, M. Bonifacic, I. Stefanic, J. Mol. Struct., 19 (1992) 267.
[51] J. Lorenc, Vib. Spectrosc. 61 (2012) 112-123.
[52] V. Krishnakumar, S. Muthunatesan, , Spectrochim. Acta A 65 (2006) 818-825.
[53] S. Subashchandrabose, N.R. Babu, H. Saleem, M.S.A. Padusha, J. Mol. Struct. 1094 (2015) 254–263
[54] N.Sundaraganesan, H.Saleem, S.Mohan, Spectrochim. Acta A 59 (2003) 1113-1118.
[55] M. Silverstein, G.C. Basseler, C. Morill, "Spectrometric identication of organic compounds", Willey, New York, 1981.
[56] G. Socrates, Infrared Characteristic Group Frequencies, John Wiley and Sons Ltd., New York, (1980).
[57] C. Ravikumar, I.H. Joe, V.S. Jayakumar, Chem. Phy. Lett. 460 (2008) 552-558.

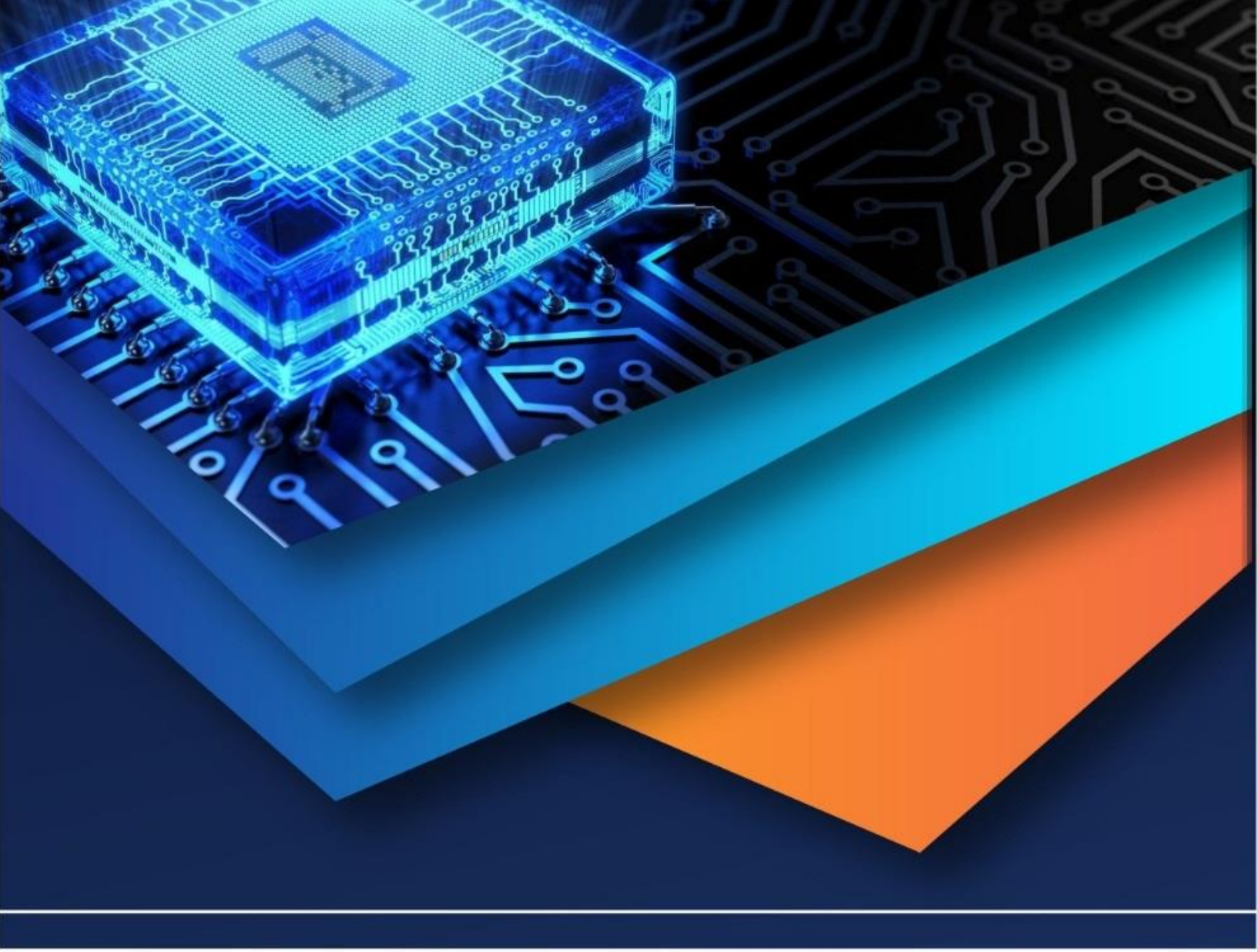

10.22214/IJRASET

45.98

IMPACT FACTOR: 7.129

IMPACT FACTOR: 7.429

INTERNATIONAL JOURNAL FOR RESEARCH

IN APPLIED SCIENCE & ENGINEERING TECHNOLOGY